Bulletin of Earthquake Engineering (2020) 18:3683–3709
https://doi.org/10.1007/s10518-020-00839-7

ORIGINAL RESEARCH

The seismic behaviour of RC exterior shear walls used for strengthening of intact and damaged frames

Hurmet Kucukgoncu[1] · **Fatih Altun**[2]

Received: 10 October 2019 / Accepted: 29 March 2020 / Published online: 7 April 2020

Abstract
Several strengthening techniques such as steel plate bonding, external post-tensioning, steel bracing, or addition of new structural elements have been widely used to improve the seismic behaviour of structures, which suffer from earthquakes. Especially, adding infill walls and shear walls to the structures are preferred because of the added increase in lateral strength and stiffness. Nevertheless, applications of these techniques have some difficulties in terms of labour, cost, usage, and comfort for occupants. Due to these difficulties, the exterior shear wall, instead of an infill wall, is applied to strengthen structures, especially for public buildings like schools, hospitals, etc. In this study, the seismic behaviours of the exterior shear walls used to strengthen intact and damaged frames were investigated experimentally. For this purpose, reinforced concrete shear walls were positioned in parallel to the exterior sides of the damaged and the intact three-dimensional frames. Both frames were tested under cyclic loads. After the investigation, the hysteresis curve, strength envelope, stiffness degradation, and the energy dissipation capacity were obtained to reveal the seismic behaviour of the strengthening exterior shear walls. In addition to these, the differences in behaviours of the shear walls applied to damaged and intact frames were identified.

Keywords Cyclic loading · Exterior shear wall · Frame · Seismic behaviour · Strengthening

1 Introduction

Many existing structures built with some deficiencies in the design or construction stage do not comply with recent code requirements in terms of strength and stiffness. Severe earthquakes have damaged many of these structures heavily and this damage leads to life and property loss. Therefore, several strengthening methods have been developed to upgrade the structures and prevent losses. These methods include section enlargement, external

✉ Hurmet Kucukgoncu
hurmet.kucukgoncu@agu.edu.tr

Fatih Altun
faltun@erciyes.edu.tr

[1] Department of Civil Engineering, Abdullah Gül University, 38080 Kayseri, Turkey

[2] Department of Civil Engineering, Erciyes University, 38280 Kayseri, Turkey

post-tensioning, external plate bonding, Ferro cement laminates, sprayed concrete, using FRP/CFRP steel bracing, or the addition of new structural elements (Hayashi et al. 1980; Rodriguez et al. 1991). One of the most common methods is adding new structural elements such as infill or shear walls to upgrade the systems (Kahn and Hanson 1979; Aoyama et al. 1984; Ersoy et al. 1998; Tezcan and Ikizogulları 1998; Yüksel et al. 2006; Erdem et al. 2006; Anil and Altin 2007; Karadogan et al. 2009; Pujola and Fick 2010; Abdel-Hafez et al. 2015; Ahmad et al. 2019). Since shear walls used as structural elements have high strength and rigidity, they are mostly applied in the structural system to resist horizontal forces in the plane of the wall and keep drifts within reasonable limits under lateral forces (Galal and El-Sokkary 2008; Husain et al. 2019). Because of significant influences, they have considerable attention not only as a structural component but also as a strengthening member to improve the capacities of lateral strength and stiffness of the strengthened structure (Higashi et al. 1980; Aoyama et al. 1984; Pincheira and Jirsa 1995; Lombard et al. 2000; Inukai and Kaminosono 2000; Tsionis et al. 2015; Alashkar et al. 2015; Chaulagain et al. 2015; and Dumaru et al. 2018). Although research in literature reveal the contribution of the structural properties of the strengthened system by adding shear walls, there have been some difficulties concerning application, cost, and time. For instance, adding the shear wall inside of the building both disturbs the occupant and prevents the usage of the buildings during the application of strengthening (Kaplan et al. 2011). Thus, it is required to apply more comfortable, practical, quick, and low- cost methods for the strengthening of inadequate structures. Therefore, a new strategy based on strengthening with an exterior shear wall has been developed to apply to structures, especially public buildings like schools and hospitals (Kaltakci et al. 2008). In many applications, reinforced concrete has been used as a structural material for shear walls (Kaltakci et al.2010, Kaltakci and Ozturk 2012), while steel and precast panels have been used in other shear wall applications (Gorgulu et al. 2012 and Kaplan et al. 2009). Additionally, the connection type between structure and shear wall can be different in terms of using anchors (Solak et al. 2015; Cirak et al. 2015). In all these studies, only the behaviour of the insufficient structure has been considered before and after a strengthening application. The strength and the rigidity of the shear wall influenced the behaviour of all systems of the shear wall, and as a strengthening member, it is important in terms of structural behaviour. In this study, two frames, which were inadequate because of some deficiencies in the construction and design stage, were strengthened with shear walls. One of the frames was selected as intact while the other was damaged in order to identify the behaviours of exterior shear walls in both situations. Finally, two reinforced concrete frames strengthened by reinforced concrete external shear walls with steel tie beams were conducted under reversed cycling loads. The results of strength, stiffness and energy dissipation were obtained to perceive differences in the structural behaviours of the external shear walls.

2 Experimental study

2.1 Description of test specimens and material properties

In the conducted experimental study, two RC shear walls on one foundation were built and tested. For strengthening the application, three-dimensional RC frames were tested, representing unsuitable cases in terms of construction and design criteria of TEC (2007) standard that were constructed as damaged and undamaged. All shear walls and frames were

1/2 scale. The height of the shear walls from the base of the wall to the top was 1500 mm, the length was 875 mm, and the thickness was 125 mm. The vertical reinforcement consisted of eight pairs of 8 mm reinforcing deformed bar, providing a reinforcement ratio of 0.8%. The lateral reinforcements of the shear walls were selected to be 4 mm in diameter spaced at 75 mm, as deformed bars in all specimens. The RC external shear walls were designed according to the TEC (2007) standard, consisting of the reinforcement ratio with other reinforcement details. The minimum aspect ratio of a shear wall was seven and correspondingly, the minimum height and width of the shear wall were 875 mm and 125 mm, respectively. Geometrical dimensions and reinforcements of all shear wall and frame specimens in each test were identical. Dimensions and reinforcement details of the specimens are illustrated in Fig. 1a, b (Kucukgoncu 2018).

All test specimens were manufactured at the same time. The ratio of the height to the length of the shear wall (*Hw/Lw*) was calculated by $Hw/Lw = 1.71$, of which behaviour was accepted as shear or sliding for short corbel shear wall behaviour according to the TEC 2007 standard (TEC 2007) for the situation that would produce bending ($Hw/Lw = 1.71 < 2$). The stiff foundations were designed to ensure fixed base conditions for both frames and the shear walls. There were two shear walls on one foundation. Both of the shear walls on the foundation were integrated into the two sides of the corner columns of the frames by using steel tie beams. The tie beams, connecting the frame and external RC shear walls, were of the preferred IPE140 profile and made with ST37 steel, as seen in Fig. 2 (Kucukgoncu 2018). The moment of inertia of the steel tie beam was selected to be less than the frame and external shear wall to increase energy consumption and provide ductile behaviour of the strengthening system. Deformed bars were used for anchorage to provide simultaneous movement of the frame and shear wall. In order to provide simultaneous movement of the frame and the shear wall between the existing frame shear walls and tie beams, a group of anchorage was applied on the frame and shear walls by using deformed bars of diameter 14 mm at the level of the beam for both sides (Burtz 2003). For this application, 15 mm holes were drilled on both beams and walls and the deformed bars were anchored in holes in the concrete with Epoxy as adhesive. An L-shaped steel plate extended along the column-beam junction was welded to the anchorage bars whereas a rectangular steel plate was welded to the face of the shear wall. The IPE 140 steel profile, to which two rows of drilled holes were bolted to the L steel profile. The steel tie beam was mounted between the frame and the shear wall by welding the steel profile to the L-shaped plates (Fig. 2).

The frame specimens were cast using low strength concrete with a compressive strength of approximately 18 MPa to represent the strength of concrete in existing buildings though the minimum concrete strength in the Turkish Earthquake Code 2007 (TEC 2007) states that it shall not be used with less than C20. However, for the exterior shear walls, the target compressive strength is preferred to be 30 MPa, in accordance with TEC (2007). Six cubes, with dimensions of $150 \times 150 \times 150$ mm, and six standard cylinders, of 150 mm in diameter and 300 mm in height, were cast during the placing of the concrete to serve as controls for the concrete strength evaluation of the frame specimens. Nine cubes and nine standard cylinder samples were cast in order to obtain the concrete strength evaluation of the exterior shear walls. For every three samples, both the cube and cylinder concrete of the frame were left in environmental conditions and the other six cube and cylinder samples were left in water to cure for 28 days. Compressive strength tests were performed on the samples and the average concrete compressive strength for all frame and shear wall specimens were obtained in the range of 18–27 and 32–42 MPa, respectively. Table 1 shows the concrete strength on the day of testing for frame and shear wall specimens.

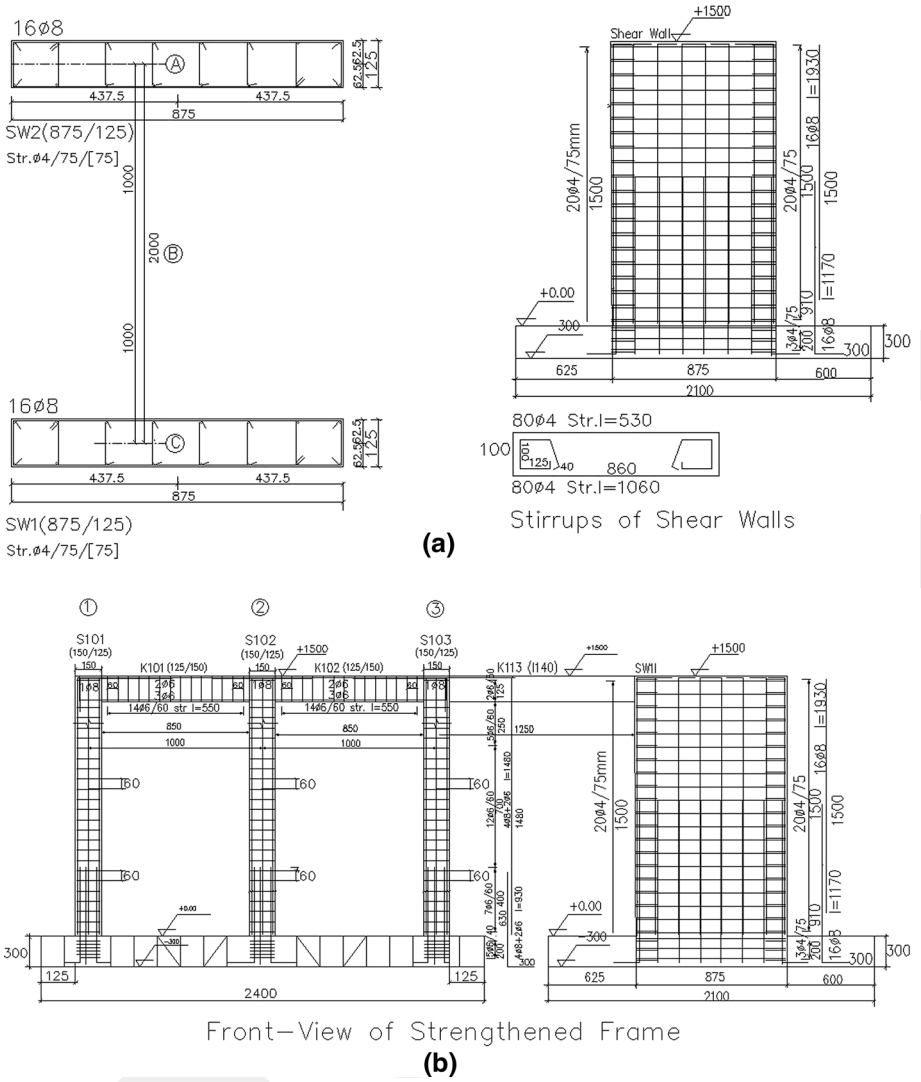

Fig. 1 Details of test specimens (Kucukgoncu 2018). **a** External shear walls, **b** external shear walls and frames

Although many codes and provisions prohibited the use of plain bars in reinforced concrete, they were used as longitudinal and transverse reinforcements since such steel plain bars were used in most of the existing building stock. The steel bars were plain in surface and were manufactured in long lengths, cut quickly, and bent without damage. In addition, they had less tensile stress than deformed bars of the same nominal size (Sacco et al. 2017). The plain bars were used for frame construction to both represent the existing building stock and to construct defective structures. However, for the construction of the shear walls as strengthening members and foundation, which provides a rigid basement, the deformed steel bars were used as is stated by the Turkish Earthquake Code 2007 (TEC 2007). The

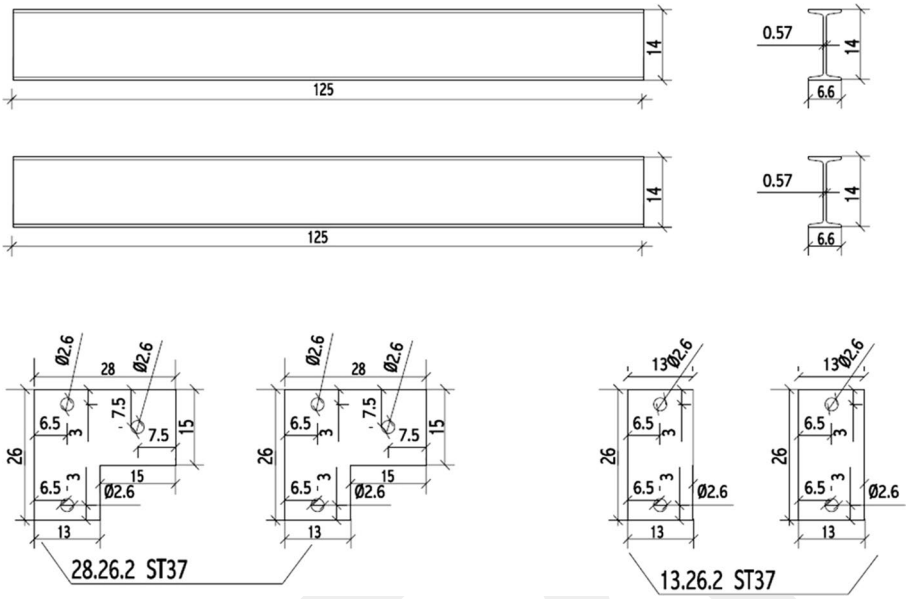

Fig. 2 Details of steel tie beams connecting to the frame and external shear wall (in mm) (Kucukgoncu 2018)

Table 1 Concrete compressive strength of frame and shear wall specimens

Specimen	Concrete cylinder strength (fc′) Mpa			Average concrete strength (fc′) Mpa	Concrete cube strength (fc′) Mpa			Average concrete strength (fc′) Mpa
FRM_Water	19.80	21.05	22.07	20.97	26.00	26.50	27.00	26.50
FRM_Environmental	17.46	18.60	18.71	18.26	18.10	18.35	18.60	18.35
SHW_Water	33.31	36.26	37.99	35.85	40.68	40.95	41.76	41.13
SHW_Environmental 1	31.37	34.45	34.65	33.49	39.70	40.00	42.20	40.63
SHW_Environmental 2	30.87	32.76	33.42	32.35	38.50	39.10	43.25	40.28

yielding strengths of the reinforcing steel bars were measured with a steel tension machine. The typical properties of both the plain and deformed steel bars are given in Table 2.

2.2 Test setup and instrumentation

The two-pairs of exterior shear walls, which were used as strengthening members for both damaged and intact RC frames, were tested, in this study. Details of the test setup, loading system, and instrumentation are shown in Figs. 3 and 4 and Table 3. The testing system consisted of a rigid floor, reaction wall, loading equipment, instrumentation, and data acquisition system. The concrete footings of all specimens were fixed to the rigid floor by steel bolts, which were 36 mm in diameter. All frames with exterior shear walls were tested

Table 2 Reinforcement properties of test frames and shear walls

Diameter (mm)	Yield strength fy (Mpa)	Ultimate strength f_u (Mpa)	Properties	Member
4	599	660	Deformed	Shear wall
6	329	458	Plain	Frame
8	321	470	Plain	Frame
8	511	624	Deformed	Shear wall
12	489	615	Deformed	Foundation
14	497	635	Deformed	Anchorage

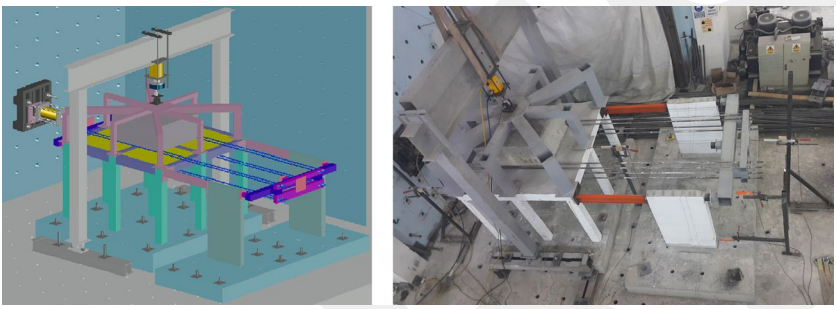

Fig. 3 View of the experimental set up of frame and external shear walls with steel tie beams

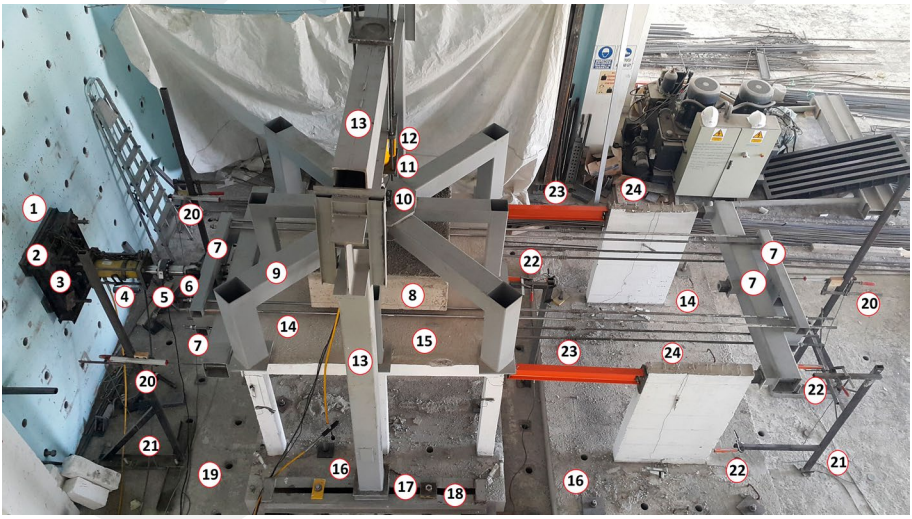

Fig. 4 Experimental set up components of the frame and external shear walls with steel tie beams

under reversed cyclic lateral loading to simulate seismic action. A lateral load was applied to specimens at each column-beam joint level using two lateral loading setups. The lateral loading setup was manufactured by assembling three different rectangular and square

Table 3 Components of the experimental set up

No.	Component	No.	Component	No.	Component
1	Rigid wall	9	Steel distribution loading set up	17	Roller bearing
2	Steel plate	10	Roller bearing	18	Steel traverse
3	Roller bearing	11	Load cell	19	Rigid floor
4	Hydraulic jack	12	Hydraulic jack	20	Potentiometer
5	Load cell	13	Steel stability frame	21	Trivet holding measurement devices
6	Roller bearing	14	Transmission shafts	22	LVDT
7	Lateral loading set up	15	Reinforced concrete frame	23	Steel tie beams
8	Concrete block	16	Steel bolts (Anchors) at the foundation	24	RC external shear walls

tubular steel profiles in different sizes. These setups were connected in the push and pull face of the bearing system by using 8 transmission shafts with 24 mm diameter at the level of the column beam joint area. A hydraulic jack, with capacities of 600 kN in compression and 420 kN in tension were mounted to a rigid reaction wall, which was used to apply the lateral load. One end of the lateral loading setup on the left side was connected to the rigid wall while the other end was connected to the frame. The end of the lateral loading setup on the right side was connected directly to the face of the shear wall. To measure the amount of applied lateral load, a load cell was integrated with the end of the jack. The applied lateral load transferred from the frame to shear walls in pull and push directions with the help of the transmission shafts.

An axial load of at least 10% of the carrying capacity was applied by hydraulic jack and was distributed from a single loader at each corner and edge columns of the frame with the help of a steel distribution loading setup while the axial load on the central column was provided by a concrete block. The steel distribution loading setup consisted of multi-leg steel construction, designed with steel profiles according to the analysis of results in the SAP 2000 software (2017). The dimensions of the profiles selected in the steel construction to provide the axial load required for each column (except middle column) were distributed in proportion to the stiffness of the profiles used in the steel construction. Hence, the axial load acting on each column was equal in the experiments. The steel distribution loading setup was hinge supported (as roller bearing). Thus, it was attempted to minimize any stiffness contribution during axial loading. The axial load produced by a single loader was measured by a load cell connected to a steel stability frame. The steel stability frame was constructed around the test frame not only to prevent out-of-plane deformations but also to carry the hydraulic jack applying the axial load and load cell measuring this load. The axial loading system consisted of the hydraulic jack connected to the steel stability frame at the top and the steel distribution system, which distributed the load to the columns just below. The steel stability frame was hinged support (as roller bearing) to provide freedom of movement during horizontal displacement to the steel stability frame.

The specimens were instrumented with the potentiometers to measure top displacements and check for torsional effect. According to the measurements from the potentiometers at the edge columns of the frames and shear walls, there was no torsion in the strengthening tests. Therefore, no changes were observed in the position of the horizontal loading mechanism during the experiments. Rigid diaphragm behaviour was expected in the test frames

where no slab opening was designed. Because of the effect of rigid diaphragm behaviour, no torsional effects, such as torsional cracks on the slabs occurred during the strengthening tests. In addition, the LVDTs (Linear Variable Differential Transformers) were placed to obtain displacements of the exterior shear walls and to check whether there was any small shifting in the foundation of the specimens. There was no shifting and no deformations were observed in the steel tie beams connected to the frames and shear walls during the tests. Displacements and the lateral and axial loads were monitored. The instrumentation scheme of the specimen is given in Fig. 5.

One of the identical frames was damaged with an up to 2.6% drift ratio, called a 'Marked Damage Region' as stated in the Turkish Earthquake Code 2007 (TEC 2007) before the strengthening application. This damage level can be also defined as a level between 'Limit State of Damage Limitation (DL)' and 'Significant Damage (SD)', as closer to the SD level, where the structure was significantly damaged with some residual strength and stiffness losses (Euro Code 8 2012). According to the Federal Emergency Management Agency (FEMA), the structural performance level of the frame can be identified as either 'Life Safety (LS) Structural Performance Level' or 'Limited Safety Structural Performance Range' defined, as the continuous range of damaged states between 'Life Safety' and the 'Collapse Prevention Structural Performance Level' due to a 2.6% drift ratio (FEMA 356 2000). In addition, moderate permanent drifts occurred, as much as 0.026 with a 40 mm horizontal displacement, with maximum deformation at an 82 kN load level. During the damaged test, crack formations occurred in the columns and flexural cracks developing towards the columns were observed in the column-beam joints. A diagonal shear crack, an X-pattern appeared in the joint area of the column when the crack widths in some beams extended to approximately 2 mm. Afterwards, the damaged and intact frames, strengthened by the exterior shear walls with steel tie beams were tested. In each experiment, in both pull and push cycles, loading history was divided into two parts. In the first part, the load-controlled loading was used until reaching the yield load and then, the displacement-controlled loading was applied. In the beginning, a 5 kN lateral load was applied to the system, including the frame and external shear walls with tie beams. The load level was maintained

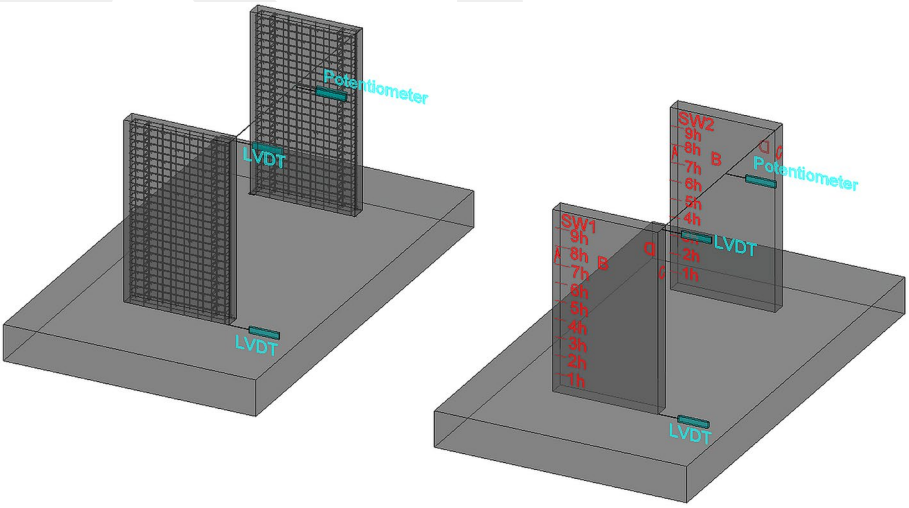

Fig. 5 Schematic representation of the instrumentation for the test specimens

in the elastic range for the first few cycles. The lateral load was increased by 5 kN in each cycle up to the 26th cycle and continued in 10 kN increments as load-controlled loading. In further cycles, the load was increased beyond the ultimate load level where the frame system reached yield point. After reaching the ultimate load-carrying capacity, deformation-controlled loading was applied with drift increments until the end of the tests. Loading histories based on lateral load and displacement are given in Figs. 6 and 7, respectively. At the end of each cycle, newly initiated cracks and crack propagations were marked on the frame and shear wall specimens. In addition, failure mechanisms were observed during the experiments.

3 Experimental results

3.1 Hysteretic behaviour of the test specimens

The performance of the shear wall specimens was evaluated through measuring the displacement and load by the LVDT, potentiometer, and load cell. For the strengthening application, two shear walls on one foundation were tested in each experiment. In the first test, external shear walls integrated in the damaged frame via steel tie beams for strengthening application were performed under reversed cycling loads. Identical external shear walls were applied to the intact frame via steel tie beams were carried out in the second test. All the results and observations refer specifically to the shear walls. After all testing, the obtained hysteresis curves, which were used to determine the strength and stiffness characteristics of the test specimens and evaluated the general behaviour of structural members, for both tests are shown in Fig. 8.

As seen in the graphs, the maximum strength of the external shear wall used for the damaged frame strengthening test was 269.55 kN while the maximum displacement of the

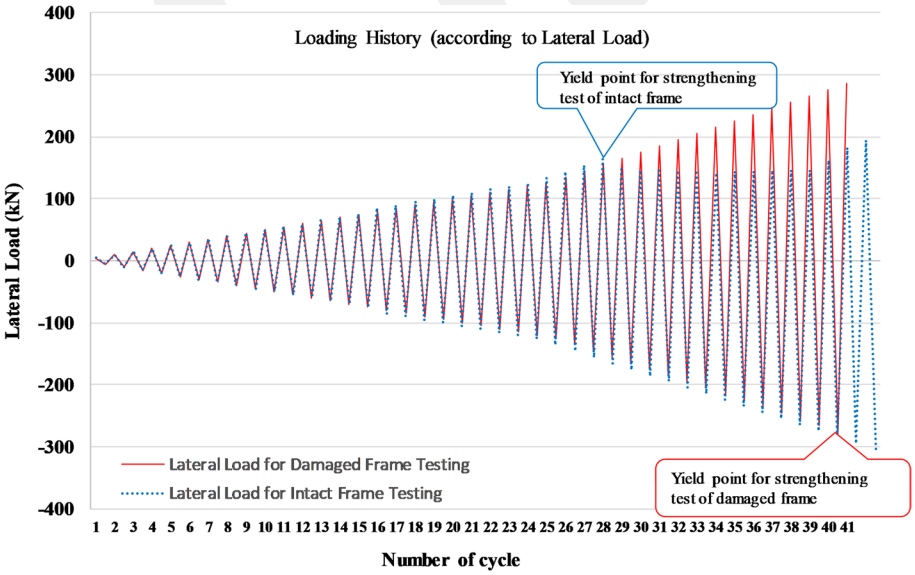

Fig. 6 Loading history of strengthening tests according to lateral load

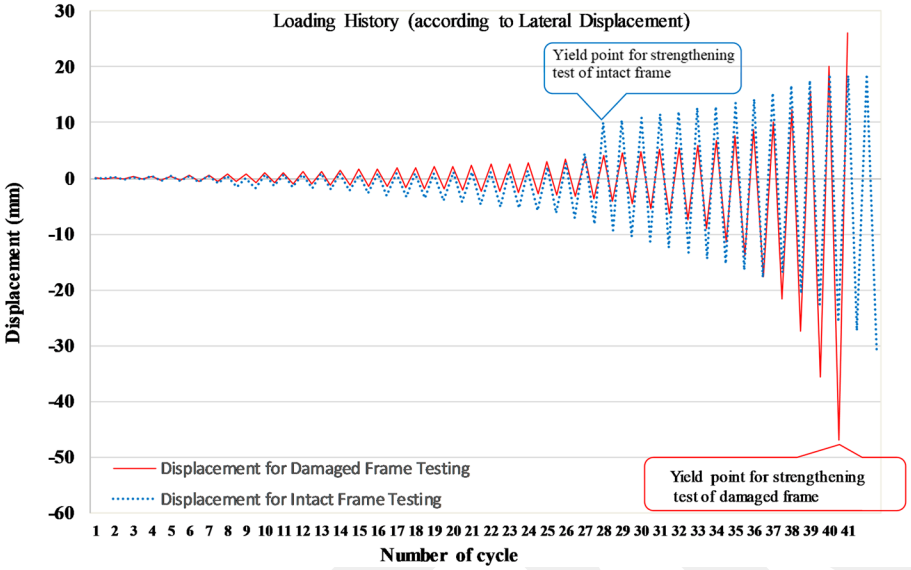

Fig. 7 Loading history of strengthening tests according to lateral displacement

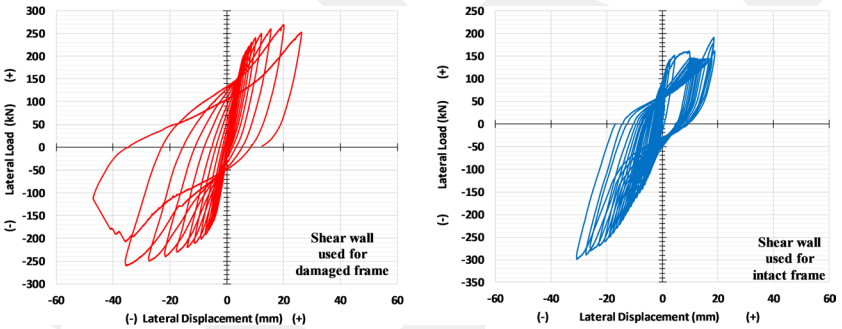

Fig. 8 Hysteresis curves of external shear walls used in both strengthening tests

shear wall was 35.48 mm. On the other side, the external shear wall used for intact frame strengthening reached 299.12 kN and 30.703 mm, as maximum strength and displacement, respectively. By comparing the results, the maximum strength of the shear wall used for strengthening of the intact frame was higher than the shear wall used for strengthening of the damaged frame. The maximum lateral displacement reaching by external shear wall used for intact frame was lower than the shear wall used for the damaged frame.

As seen in Fig. 8, during the elastic behaviour of the strengthening system before the yielding limit, the displacements in the push and pull cycles were close to each other. The displacement differences in the push and pull cycles became more significant during the inelastic behaviour after the yielding limit. Therefore, the displacement differences between the push and pull cycles were numerical quantities that might arise due to the effect of plastic hinges, which occurred during the push and pull cycles. In addition, the symmetries of curves obtained from the strengthening test were distorted due to the differences

in interaction between the shear wall behavior with high rigidity and frame behaviour with low-rigidity. This is because the moment of inertia of the steel tie beam was selected to be less than the frame and external shear wall to increase energy consumption and it provided the ductile behaviour of the strengthening system. Since the load distribution was affected in the pull and push cycle due to the low moment of inertia of the steel tie beam, the symmetry in the curve was distorted.

The lateral load acting on both frame and shear walls was measured by the load cell while the lateral displacements of the frame and shear wall were measured by the potentiometer and LVDT located at the joint of the frame and shear wall along the same axis. The applied lateral load transferred from the frame to shear walls in the pull and push cycles with the help of the transmission shafts. The measurements obtained from these points are shown in Fig. 9 as lateral load–displacement curves. According to the results, the lateral load level acting on each of the shear walls was the same as the frame specimen in each strengthening test. In addition, the horizontal part of the curves in the hysteresis diagram was observed due to permanent displacement that was caused to occur by crack development.

An increase in the hysteresis curve of the shear wall appeared due to the compression in the hinges and bolts coupled in the steel tie beams during the intact frame-strengthening test, especially in the pull cycles. In addition, the moment of inertia of the steel tie beam was selected as less than the intact frame and the external shear wall to increase the energy consumption and ductile behaviour of the strengthening system. From that point on, the exterior shear wall behaviour dominated the system behaviour, significantly. Therefore, both the moment of inertia of the steel tie beam and the clamping affected differences in the distribution of forces between the frame and shear walls as both global and local responses and the caused structural behaviour was predominated by the shear walls.

3.2 Shear wall specimen behaviour and failure mechanism

During all tests, the behaviours of the shear walls, including damage and crack patterns, were monitored. Each shear wall was divided into 150 mm intervals, referred to as ‘h’ from bottom to top in order to observe crack propagation. In this study, ‘h’ represented the column dimension along the loading direction. In addition, the faces of the shear walls were named, beginning from the loading face counterclockwise as A, B, C, and D, respectively

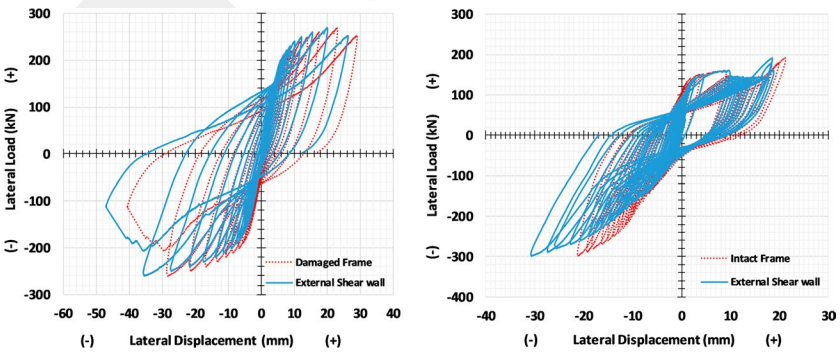

Fig. 9 Lateral load–displacement curves for the distribution of lateral load between frames and external shear walls in the damaged frame and intact frame strengthening tests, respectively

(Fig. 5). Also, the shear wall labelled with SW1 was indicated as front shear wall, whereas the shear wall labelled with SW2 was called as back shear wall in crack development expression. All cracks occurring in the push cycles were marked blue while the cracks in the pull cycles were marked red.

The first experiment was strengthening of the damaged frame using external RC shear walls with steel tie beams. The first crack on the shear walls was observed on the 1 h and 2 h levels of the C face of the front shear wall at a 195 kN load level during the 32nd push cycle. In the 37th pull cycle at 245 kN, some flexural cracks on the B face of the front shear wall started from the 2 h level to the 3.5 h, 4 h, and 4.5 h levels, whereas on the C and D faces of the same shear wall at the 2 h, 2.5 h, and 4 h levels cracks were detected. In the same cycle, similar cracks were recorded on the B face of the back shear wall at the 1.5 h, 3.5 h, and 4.5 h levels and on the C and D faces of the back shear wall at the 0.5 h, 1.5 h, 2 h, 3 h, and 3.5 h levels flexural cracks were observed. As existing crack widths were expanding in the 38th push cycle, new crack formations were noted on both the pull and push faces of the front and back shear walls. The cracks on the B face of the front shear wall were recorded at the 0.5 h, 2 h, 3 h, and 4 h in the 39th push cycle at 265 kN. In addition to new cracks, the crack width in the base-wall joint area of the front shear wall reached 6 mm. There was an observation that the concrete cover on the base-wall joint area of the back shear wall spalled. Since the anchorage connections between the RC frames and external shear walls were also monitored regularly during the testing, there was deboning along with the anchorage of steel tie beam connecting the damaged RC frame and back shear wall after the 39th cycle. Additionally, in this area of the two-shear walls, the crack formation condensed due to the working of the anchorage of the steel tie beam after the 30th cycle. The separation along with both the front and back walls in the base-wall junction area became more apparent and the opening reached approximately 15 mm in the 39th cycle. In the same cycle, when the concrete cover on the C side of the front wall spalled, the reinforcing bars in that area were visible. Buckling in the longitudinal reinforcement, which was located between the base and the floor of the front and back walls were observed in the 40th push cycle. When the cycle reached the 40th pull, the longitudinal reinforcements in the wall-base joint on the C face of the back shear wall ruptured and the shear cracks opened significantly (Fig. 10). After that, the lateral load decreased to 130 kN and the displacement of the shear wall suddenly reached 47 mm. As the width of opening and separation in the base-wall joint increased, the right corner of the back shear wall along the side of the B face partially pulled away (Fig. 10). In the last cycle, the test was terminated by resetting the load before the shear wall failed from the base.

The second test was strengthening of the intact frame via external RC shear walls and steel tie beams. The first crack was observed on the back shear wall at the 1 h level starting from the B face, then propagating to the B-C corner, and continuing along the D face at the 70 kN load level in the 14th push cycle. Then, a flexural crack on the front external shear wall was observed on the B face at the 1 h level, in the 15th push cycle at 75 kN. In the 21st push cycle at a 110 kN load level, a flexural crack on the front shear wall was noted on the B face at the 1–2 h levels. In addition, similar flexural cracks occurred on the B, C, and D faces of the back shear wall at the 1–2 h levels. When the 30th push cycle was carried out, the cracks on faces B and C of the front shear wall starting from the 1–2 h levels continued to the 3 h and 4 h levels were recorded at a 235 kN load level. On the back external shear wall, there were two flexural cracks on face B at the 1–2 h and 3 h levels while on the C and D faces, they were at the 1 h and 1–2 h levels. In addition, the crack on the C face of the back shear wall occurred in the same cycle. After the 35th cycle, the cracks on the B face of the front shear wall starting from the 2 h and 3 h levels continued downwards. The

Fig. 10 Buckling of the reinforcement of the shear walls and separation at the base of the shear wall in strengthening of the damaged frame test

four transverse cracks on the B face of back shear wall propagated, starting from above the 4 h level to 4 h, 4 h to 3 h levels, 3 h to 2 h levels, and finally 2 h to 1 h levels. In addition, the crack on the D face of the same shear wall fell away from the 4–5 h levels to just below the 4 h level while other cracks on the same face of the same wall spread out from the 3 h level to 2 h level. It was observed that there was a significant separation at the base-wall junction on the B face of the front shear wall in the 38th cycle. In the 40th cycle at a 285 kN load, the flexural cracks on face B of the front shear wall occurred from the 7 h level and fell away toward the 3 h level. In addition, two-crack formations on the same face of the same wall were monitored from the 5–6 h levels and 5 h level falling away to the 3 h level. On face D of the back shear wall, some crack propagations beginning from the 6–7 h levels to the 4–5 h levels, the 5–6 h levels to the 3–4 h levels, and the 4 h level to the 3 h level were observed in the same cycle. In the 41st cycle, when the concrete cover on the wall-base joint at B-C corner of front shear wall spalled, the reinforcement in this area clearly appeared. It was observed that the separation and opening, which started from the wall-base junction area of face B of the front shear wall was observed more apparently. When the 42nd cycle was performed, there was buckling in the longitudinal reinforcement at the baseline of face C of the front shear wall. Also, due to the opening between the bottom of the front shear wall and the base joint, starting from the right corner of the shear wall to along the side of the front face, the front shear wall failed at about 300 kN by reaching 38 mm as peak displacement (Fig. 11).

It was checked whether the anchors connecting the frames and external shear walls with steel tie beams peeled or opened during the experiments. During these inspections, especially after the 30th cycle in the damaged frame strengthening test, due to the work of the anchors of the steel tie beams connecting the frames and external shear wall, crack intensity increased in the column-beam joint section and some peeling was observed in the anchors

Fig. 11 Buckling of the reinforcement of the shear walls and separation at the base of the shear wall in the strengthening of the intact frame test

(Fig. 12). Some microcracks occurred in the same section of the intact frame strengthening test but the intensity of the cracks were less than those of the damaged frame strengthening test. Nevertheless, there was no damage in any steel tie beams in the strengthening tests.

4 Discussion of the test results

4.1 Strength of the external shear walls

Strength envelopes for the external shear wall specimens shown in Fig. 13 were plotted by connecting the peak points of lateral load displacement hysteretic curves at two cycles for each specimen.

As seen in the graphs, the ultimate loads of external shear wall recorded during the pull and push cycles for the strengthening test of the damaged frame were 269.55 kN and 260.36 kN while those obtained from the strengthening test of the intact frame were 191.40 kN and 299.12 kN, respectively (Table 4). Maximum displacements in the pull and push cycles of the shear wall used in the damaged strengthening tests were 26.26 mm and 35.48 mm, respectively. In addition, the maximum displacement in the pull and push cycles of the intact frame strengthening test were noted as 18.53 mm and 30.70 mm, respectively. This means that the shear wall used to strengthen the intact frame had 14.89% more strength than the shear wall used in the strengthening test of the damaged frame. However, the maximum displacement of the shear wall applied to the damaged frame was calculated as 1.16 times higher than that used in the testing of the intact frame. According to results, higher strength was observed in the shear wall specimen used for the strengthening test of the intact frame while the lower displacement of the shear wall was noted for the same test. The behaviour of the shear wall used for the damaged frame was observed almost similar to the shear wall applied to the intact frame. Nevertheless, the shear wall applied to the intact frame had more strength and less displacement due to the behaviour and rigidity of the intact frame. This means that the intact frame had much higher strength than the damaged frame. Therefore, the strength of shear walls in the strengthening test were affected by the strength of the frames and the frame behaviour.

4.2 Stiffness and ductility

The degradations of stiffness for all the specimens are shown in Fig. 14. Tangent (initial) stiffness is defined as the initial slope of the lateral load-top displacement curve.

Fig. 12 The anchors for the steel tie beams in the damaged frame strengthening test

Secant (maximum load) stiffness is defined as the mean of the slope of the lines connecting the origin to the peak points of the maximum load obtained for both pull and push cycles. Collapse (failure load) stiffness is defined as the mean of the slope of the lines connecting the origin to the peak points of the collapse load obtained for both pull

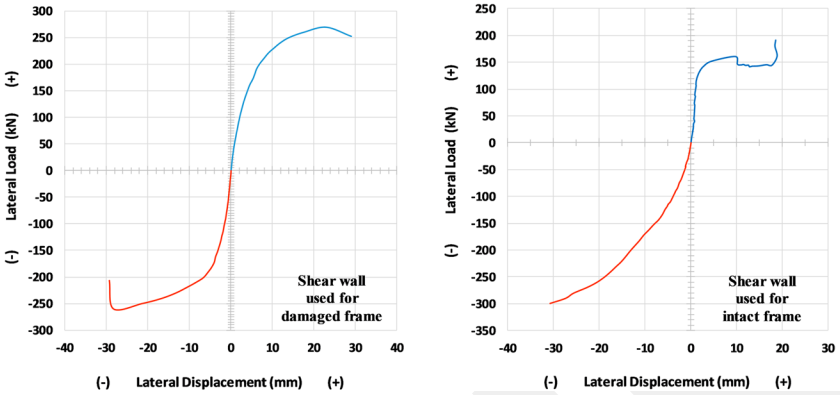

Fig. 13 Strength envelopes of the external shear walls used in strengthening testing

and push cycles (Kaltakci and Yavuz 2014). Accordingly, the tangent stiffness, secant stiffness, and collapse stiffness values of the test specimens are listed in Table 4.

The tangent stiffness of the external shear walls used for strengthening of the damaged and intact frame were calculated as 74.955 kN/mm and 63.318 kN/mm, respectively. In addition, the secant stiffness calculated from the strengthening test of the damaged frame was 9.615 kN/mm, whereas the strengthening test of an intact frame was 9.962 kN/mm. Finally, the collapse stiffness was determined as 8.596 kN/mm in the damaged frame strengthening test while it was calculated as 9.962 kN/mm in the intact frame strengthening test. Accordingly, the shear wall used for strengthening of the damaged frame had larger stiffness degradation (88.53%) than the shear wall used for the strengthening of the intact frame (84.27%) during the tests.

After the calculation of the stiffness values, it was noticed that the tangent stiffness of the external shear wall used for strengthening of the damaged frame was 1.18 times higher than the intact frame strengthening test, surprisingly. The main reason for the damaged frame having less stiffness was due to damage and crack developments in the frame. Although the rigidity was decreased with the development of cracks in the damaged frame, the high stiffness measured in the first loading cycle was caused by the stiffness of uncracked external shear wall, since the system was exposed to permanent displacement. Thus, the external shear walls dominated the behaviour, especially at the beginning of the test. Then in further cycles, the system including both the frame and external shear walls jointly dominated the behaviour. However, the secant and collapse stiffness of the shear wall used in the intact frame strengthening test were higher than the other test, as expected. Yet, there were no significant differences between the stiffness values due to the system behaviour. The stiffness degradation is the ratio of the tangent stiffness value to the collapse stiffness value.

Displacements at ultimate points where the load fell to 80% were used with the yield displacements in the evaluation of ductility. A graphical method was used to obtain the ductility values of the shear walls utilizing the envelope curves in the hysteresis diagrams. In this method, the displacement (Δu) at the ultimate point where the load fell to 80% because the response spectrum of the shear wall specimens did not intersect the spectrum curve in the Acceleration Displacement Response Spectrum diagram for the displacement-based design. Yield displacement (Δy) was calculated by the intersection of the lines,

Table 4 Lateral load bearing capacity, stiffness, and displacement ductility values of external shear wall specimens

Test specimen	$F_{ultimate}$ (kN)	δ/H		Stiffness (kN/mm)			Stiffness degradation	Ductility						
		Max. load	Last cycle	Initial load	Max. load	Failure load	%	Push			Pull		Average	
								Δ_{max} (mm)	Δy (mm)	μ	Δy (mm)	μ	$\Delta y_{avg.}$ (mm)	μ_{avg}
Shear wall used for damaged frame	269.55	0.0237	0.0133	74.955	9.615	8.596	88.53	19.95	14.56	1.37	26.62	1.33	20.54	1.35
Shear wall used for intact frame	299.12	0.0205	0.0205	63.318	9.962	9.962	84.27	18.83	18.65	1.01	17.06	1.03	17.86	1.02

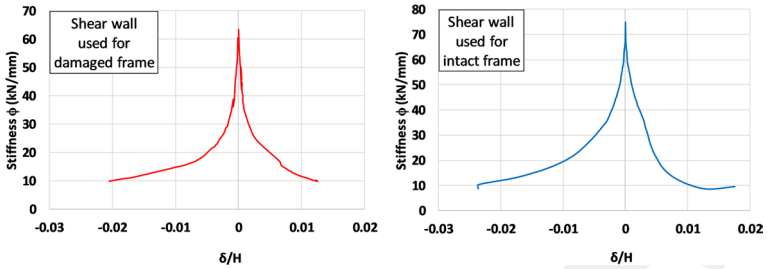

Fig. 14 The degradation of stiffness for external shear walls

which combine the coordinates of the peak point cycle (F_{max}, Δ_{max}) and the coordinates of the second previous cycle from the peak point cycle (F_{max-2}, Δ_{max-2}), graphically. Then, the ductility values of the shear walls were calculated for both the push and pull cycles by using the formulation ($\mu = \Delta u/\Delta y$) (Dirikgil and Atas 2019). The ductility values of the strengthening external shear walls are given numerically in Table 4. In addition, the mean ductility values were calculated by the values from the push and pull cycles for comparison. Although the displacement value of the external shear wall used for intact frame was higher than the damaged frame, the mean displacement ductility value calculated from the shear wall in the damaged frame strengthening test was greater than the shear wall in the intact frame. As seen in Table 4, by the increment in the stiffness degradation of the shear walls, ductility was found to increase as well. When the displacement ductility values of the shear walls were investigated, it was noticed that the damaged frame behaviour also played an important role due to crack formation with the shear wall in terms of mean displacement ductility.

4.3 Energy dissipation

The energy dissipation capacity of structural system components is an important indicator affecting the behaviour of structures in earthquakes. Structural members with plastic behaviour dissipate some energy per cycle of loading. The concepts of energy dissipation and stored plastic energy are related to elastic and plastic straining theorems, the heterogeneous nature of deformations, and cracks in the micro-mechanical level. The energy terms are categorized into elastic and plastic energy in the structure during reversed cycling loading (Collins 2005). Elastic energy is recoverable when it unloads to original imposed stress conditions represented by the pink shaded area in Fig. 15. Although stress changes in the micro-mechanical level, elastic straining at that level is not likely to be recovered. This energy is called unrecoverable plastic energy when considering macro-mechanical behaviour. For reversed cycling loading, the energy dissipation rate was evaluated from the area under the envelope curves plotted as the measured load versus displacement curve. The term consumed energy means unrecoverable mechanical work, which was supposed to include all irreversible parts of the work done, was calculated by the total area under the A, B, C, D, E, F, and G points in Fig. 15. The energy stored in the structural member is defined as stored energy by adding up recoverable elastic energy and unrecoverable plastic energy (Fig. 15).

The energy dissipation of the specimen was obtained by calculating the areas inside the hysteretic load–displacement loops for each cycle. The consumed cumulative energy was

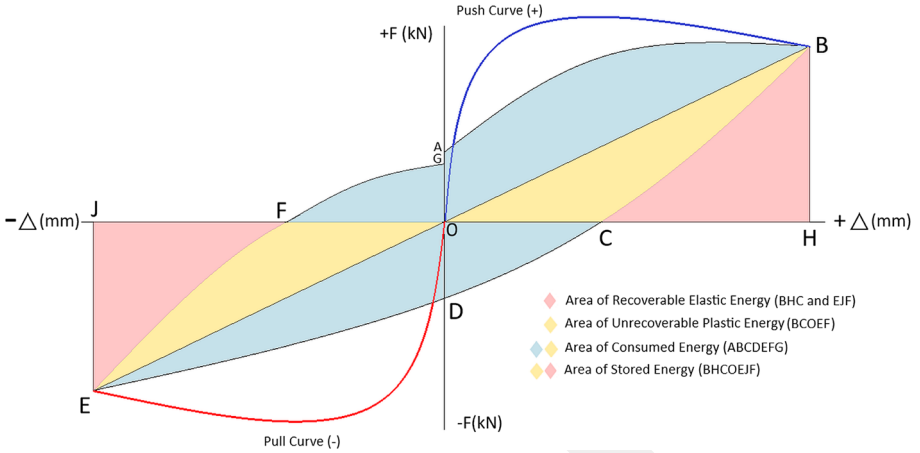

Fig. 15 Energy consumption zones (Dirikgil and Atas 2019)

calculated by adding the energy dissipated in successive cycles during the test. In addition to this, the calculation of the energy stored per cycle, the recoverable elastic, and unrecoverable plastic energy per cycle for each specimen are shown in Figs. 16 and 17. In addition, the amounts of the energy per cycle of shear wall in both tests are given in Fig. 18, comparatively.

As seen from the graphs, the amount of consumed energy of the shear wall used for the strengthening of the damaged frame was calculated as 68,084 kN-mm, whereas the same energy value was obtained as 42,173 kN-mm for the shear wall used for the intact frame. The stored energy was determined as 42,212 kN-mm while it was calculated as 54,372 kN-mm in the strengthening test of the intact frame. Moreover, the amount of elastic energy of the shear wall used in the testing of the damaged frame was 19,629 kN-mm while the amount of plastic energy was 22,583 kN-mm. Otherwise, the amount of

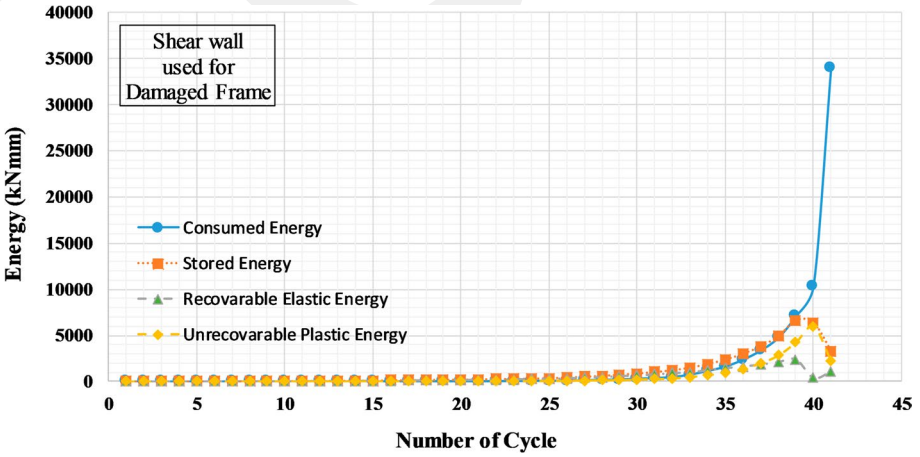

Fig. 16 Energy values of the shear wall used in the strengthening test of the damaged frame

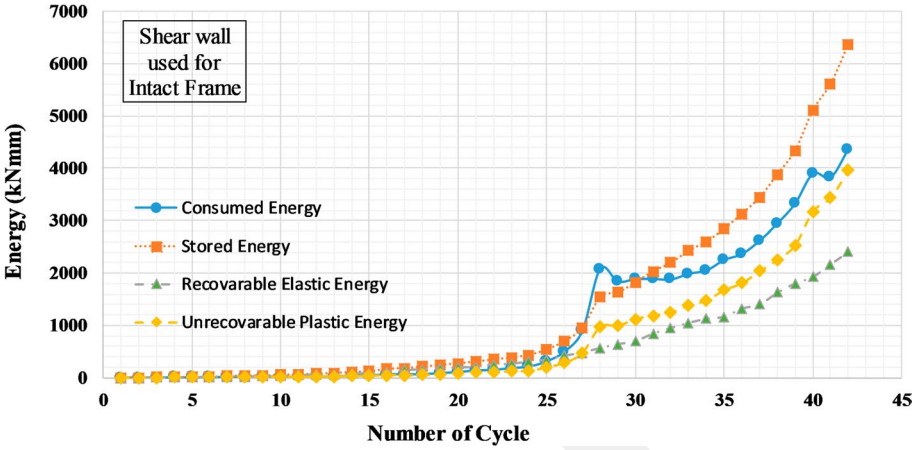

Fig. 17 Energy values of the shear wall used in the strengthening test of the intact frame

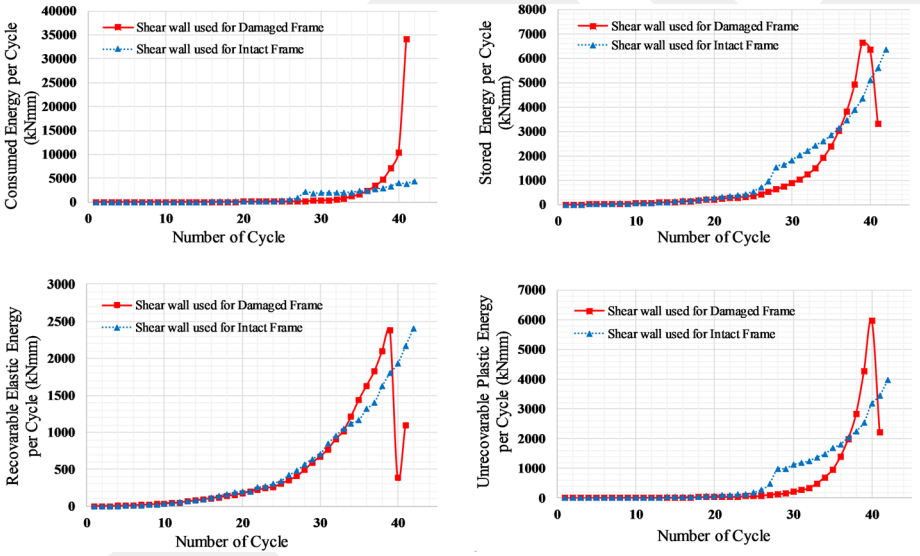

Fig. 18 Energy values of the shear walls used in the strengthening test

elastic energy of the shear wall for the strengthening of the intact frame was calculated as 23,241 kN-mm and the amount of plastic energy was estimated as 31,131 kN-mm.

The consumed energy per cycle of the shear wall used for the damaged frame was 148.22% higher than the shear wall used for the intact frame. The amount of stored energy per cycle of shear wall in both tests was close as expected in the last cycle, where the stored energy of the shear wall used for the damaged frame dropped suddenly due to a failure mechanism. Recoverable plastic energy per cycle was similar in each test but identically, in the last cycle, there was a sudden drop in the strengthening of the damaged frame testing. However, it was observed that the unrecoverable plastic energy per cycle of the shear wall

used for the damaged frame was greater than the intact frame. As a result of this, it was supposed that the higher amount of energy dissipation observed in the shear wall was in the strengthening of the damaged frame testing due to the ductile behaviour of the system. The reason was that the shear walls consumed energy while cracks were opening and closing during the cycles throughout the testing. Another reason was the decreasing rigidity of the damaged frame affecting the external shear walls. Figure 19 depicts the variation of cumulative dissipated energy as a function of drift ratio. Energy consumption graphs, depending upon the δ/H ratio, are presented for better comparison (Fig. 19).

Total energy values of the shear wall specimens are shown in Table 5. According to the energy data values obtained at the end of the testing, the consumed energy value of the shear wall in strengthening testing of the damaged frame was calculated as higher than the testing of the intact frame. On the contrary, the stored energy value of the shear wall in the same testing was lower than the other test. Moreover, recoverable elastic and unrecoverable plastic energy of the shear wall used for the intact frame was higher than the damaged frame.

As the energy consumed during the test also related to the number of cycles, the energy consumed in the cycle where the lateral load reached maximum capacity was a useful parameter for comparison. Therefore, the dissipation energy of maximum lateral load is shown in Table 5. In Table 5, the amounts of stored, recoverable elastic, and unrecoverable plastic energies were higher in the shear wall used for the intact frame than the damaged frame. Yet, the largest amount of consumed energy was in the shear wall used for the damaged frame. In conclusion, the damaged RC frame strengthened by RC external shear walls with steel tie beams consumed more energy under a cyclic load than the intact RC frame due to both cracks and damage that opened and closed during the cycles and its low rigidity. Decreasing rigidity of the damaged frame affected the amount of energy that was consumed by the shear walls.

4.4 Crack and damage pattern

During both tests, flexural crack patterns on the push and pull faces of all external shear walls were observed. Opening in the shear wall-base joint occurred in further cycles as the width of the opening expanded and then turned into significant separation. As a result, the external shear walls failed. It was determined that the failure mechanism was shear failure due to a collapse, which had occurred at the baseline of the shear walls. According to a comparison between the strengthening of damaged and intact frames via external shear walls, the first crack patterns on the external shear walls appeared in the strengthening of the intact frame. However, an opening along the baseline of the shear

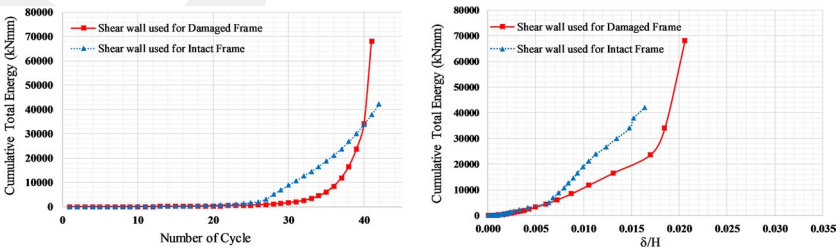

Fig. 19 Cumulative energy values versus number of cycle and drift ratio of the shear wall specimens

Table 5 Total energy data calculated for shear wall specimen

Test specimen	Consumed energy Et (kN-mm)		Stored energy Ed (kN-mm)		Recoverable elastic energy (kN-mm)		Unrecoverable plastic energy (kN-mm)	
	Max. load	End of test	Max. load	End of test	Max. load	End of test	Max. load	End of test
Shear wall used for damaged frame	34,042	68,084	3315	42,212	1091	19,629	2224	22,583
Shear wall used for intact frame	4364	42,173	6366	54,372	2404	23,241	3962	31,131

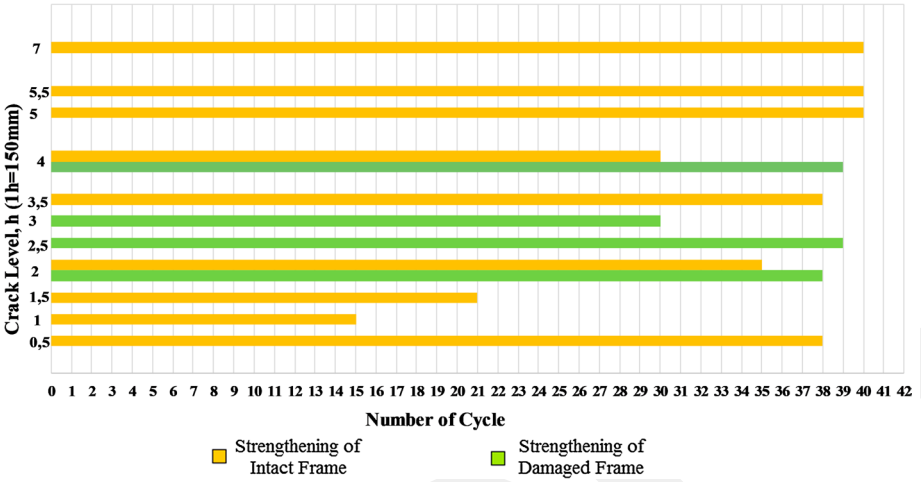

Fig. 20 Crack propagation on the pull face of the front shear wall

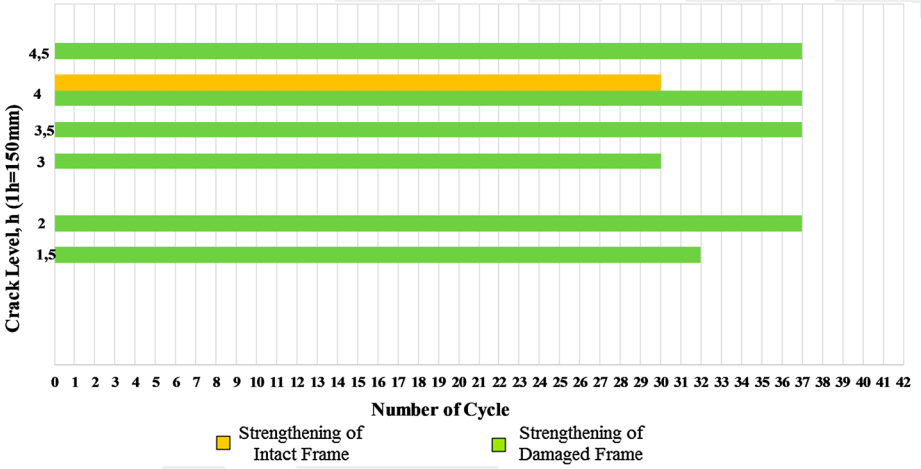

Fig. 21 Crack propagation on the push face of the front shear wall

wall occurred in further cycles. In addition, the crack density on the external shear wall used in the strengthening of damaged frame testing was more than in the strengthening of intact frame testing. Although buckling in the longitudinal reinforcement at the wall-base junction area of the external shear walls was observed in the two strengthening tests, the amount of buckled reinforcement bar of the shear wall in the damaged frame test was higher than the intact frame test. As the amount of buckled longitudinal reinforcement bar in the wall-base junction increased, most of the reinforcement bar located in this joint area suddenly ruptured. Because of rupturing in the reinforcement bar, friction shear strength decreased and shear failure mechanism appeared as shown in Figs. 20, 21, 22 and 23. In the study, each shear wall was divided into 10 intervals (each interval was 150 mm) represented as 'h' from the bottom to the top to monitor crack

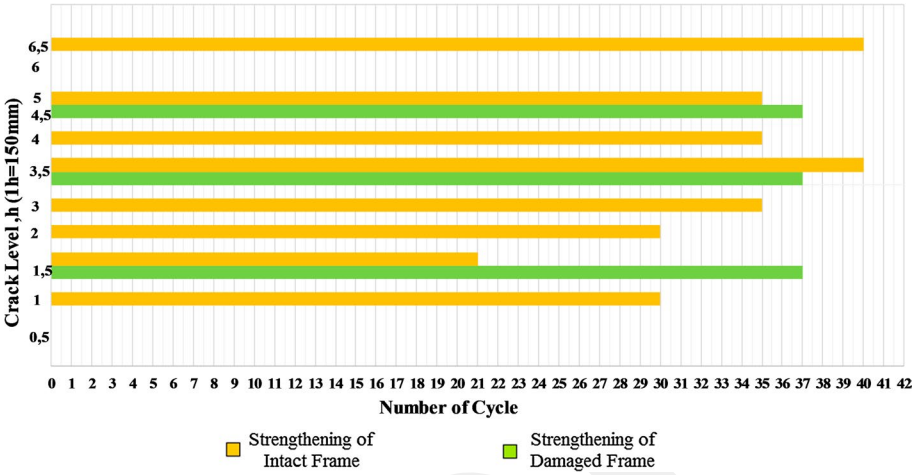

Fig. 22 Crack propagation on the pull face of the back shear wall

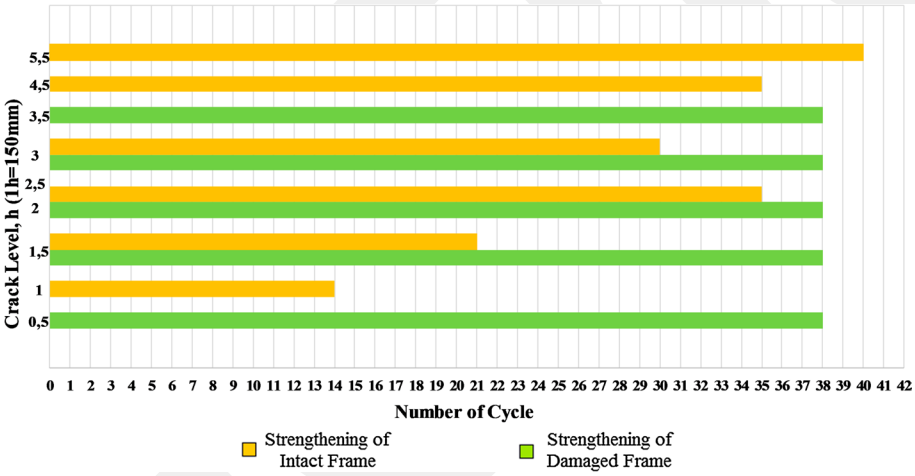

Fig. 23 Crack propagation on the push face of the back shear wall

formation. This is seen in Fig. 5. Figures 20, 21, 22 and 23 shows the cracks, which appeared in these interval levels represented by 'h' on the shear wall faces.

5 Conclusion

In this study, an experimental investigation on seismic behaviour of an exterior RC shear wall, used for strengthening of RC damaged and intact structures, was carried out. One-bay, one-story reinforced concrete frames, equipped with design and implementation defects and four exterior RC shear walls, with steel tie beams, were tested under reversed

cyclic loading simulating seismic action. The following conclusions were draw in light of the 1/2-scale tests reported in this paper:

- The strength of the shear wall used for the strengthening test of the intact frame was higher than the strengthening test of the damaged frame while the displacement capacity of the shear wall used with the intact frame was lower than the shear wall used with the damaged frame due to the strength of the frame.
- The initial stiffness of the shear wall used in the damaged frame was higher compared to the shear wall used in the intact frame for strengthening. Thus, the stiffness of the external shear wall affected the system stiffness due to the low stiffness of the damaged frame. However, the stiffness at the maximum and failure load levels of the shear wall used in the intact frame were higher than the shear wall used in the damaged frame testing due to the rigidity of the intact frame.
- Despite the displacement capacity of the external shear wall in the strengthening test of the intact frame being higher than the damaged frame, the mean ductility value of shear wall integrated with the damaged frame was greater than the shear wall used for the intact frame.
- When the energy capacities of the external shear walls obtained during the tests were examined, the amounts of consumed and unrecoverable plastic energy per cycle of the shear wall used for strengthening of the damaged frame were larger than the shear wall used in the intact frame testing. The amounts of stored and recoverable elastic energy per cycle of the shear wall for the strengthening of the damaged frame were smaller than the shear wall of the intact frame test as expected. At the end of the tests, the amount of cumulative total energy of shear wall used for the damaged frame was obtained as a larger value as compared to the shear wall used for strengthening of the intact frame. A reason for this case can be shown by the amount of the consumed energy increased as cracks on the damaged frame opened and closed during the forward and backward cycles throughout the test.
- As the crack formations of the external shear walls were evaluated, a flexural crack that appeared on the baseline of the shear wall during earlier cycles, opened wider in further cycles. Then, longitudinal reinforcement in this area ruptured because of the buckling. Shear slip occurred at the base of the shear wall by decreasing frictional shear strength due to shear failure. In addition, it was observed that despite the cracks occurring on the shear wall used for the damaged frame enlarged rapidly, the crack intensity on the shear wall used for the intact frame increase more than the shear wall used in the damaged frame testing. The shear wall used for strengthening the damaged frame reached shear failure mechanism more swiftly.

The seismic behaviour of the shear wall used for the intact reinforced concrete frame had more strength, rigidity, and displacement capacity than the shear wall used for the damaged frame at the end of the experiments. The ductility and dissipated energy values of the external shear wall used for the damaged frame were higher than the shear wall used for the intact frame. In literature, previous studies indicated that the strengthening method of external shear walls made a significant contribution to the frame in terms of lateral load-bearing capacity, rigidity, and energy dissipation capacity according to experimental results (Kaltakci et al. 2008; Kaplan et al. 2011; Kaltakci and Ozturk 2012; Gorgulu et al. 2012). This study showed that the structural behaviour of the exterior RC shear walls used for strengthening of the damaged and intact frames were affected by the behaviour of the frames. Therefore, the shear walls used for both damaged and intact frames to strengthen

have different capacities in terms of strength, stiffness, ductility, and energy consumption. However, this is a desirable feature for a strengthening application as it shows that both the frame and the external shear walls cooperate against seismic action even if steel tie beams were used.

Acknowledgements This study was conducted at the Structural Mechanics Laboratory of Erciyes University. The research presented in this study was supported financially by the Department of Scientific Research Projects at Erciyes University (Project No.: FDK-2017-7722).

References

Abdel-Hafez LM, Abouelezz AEY, Elzefeary FF (2015) Behavior of masonry strengthened infilled reinforced concrete frames under in-plane load. HBRC J 11(2):213–223. https://doi.org/10.1016/j.hbrcj.2014.06.005

Ahmad N, Akbar J, Rizwan M, Alam B, Khan AN, Lateef A (2019) Haunch retrofitting technique for seismic upgrading deficient RC frames. Bull Earthq Eng. https://doi.org/10.1007/s10518-019-00638-9

Alashkar Y, Nazar S, Ahmed MA (2015) Comparative study of seismic strengthening of RC buildings by steel bracings and concrete shear walls. Int J Civ Struct Eng Res 2(2): 24–34. ISSN 2348-7607

Anil Ö, Altın S (2007) An experimental study on reinforced concrete partially infilled frames. Eng Struct 29(3):449–460. https://doi.org/10.1016/j.engstruct.2006.05.011

Aoyama H, Kato D, Katsumata H, Hosokawa Y (1984) Strength and behavior of post cast shear walls for strengthening of existing R/C buildings. In: 8th world conference on earthquake engineering, San Francisco CA, pp 485–492

Burtz JL (2003) Behavior and design of grouted anchors loaded in tension including edge and group effects and qualification of engineered grout products. Master Thesis, University of Florida, USA

CEN (2012) Eurocode 8: Seismic design of structures for earthquake resistance—Part 3: assessment and retrofit of buildings. Corrigendum, Brussels

Chaulagain H, Rodrigues H, Spacone E, Varum H (2015) Assessment of seismic strengthening solutions for existing low-rise RC buildings in Nepal. Earthq Struct 8(3):511–539. https://doi.org/10.12989/eas.2015.8.3.511

Cırak IF, Kaplan H, Yılmaz S, Degirmenci CO, Cetinkaya N (2015) A model for shear behavior of anchors in external shear walled frames. Res Eng Struct Mater 1(2):53–71

Collins IF (2005) The concept of stored plastic work or frozen elastic energy in soil mechanics. Geotechnique 55(5):373–382

Dirikgil T, Atas O (2019) Experimental investigation of the performance of diagonal reinforcement and CFRP strengthened RC short columns. Compos Struct 223:1. https://doi.org/10.1016/j.compstruct.2019.110984

Dumaru R, Rodrigues H, Varum H (2018) Comparative study on the seismic performance assessment of existing buildings with and without retrofit strategies. Int J Adv Struct Eng 10:439–464

Erdem I, Akyuz U, Ersoy U, Ozcebe G (2006) An experimental study on two different strengthening techniques for RC frames. Eng Struct 28(13):1843–1851. https://doi.org/10.1016/j.engstruct.2006.03.010

Ersoy U, Ozcebe G, Tankut T, Turk M, Sonuvar O (1998) Behavior of reinforced concrete infilled frames: an experimental study. In: Second Japan—Turkey Workshop on Earthquake Engineering, 1998, İstanbul, Turkey, pp 292–308

FEMA 356 (2000) NEHRP Guidelines for the seismic rehabilitation of buildings. Federal Emergency Management Agency, Washington DC

Galal K, El-Sokkary H (2008) Recent advancements in retrofit of RC shear walls. In: The 14th world conference on earthquake engineering, 2008, Beijing, China

Gorgulu T, Tama YS, Yilmaz S, Kaplan H, Ay Z (2012) Strengthening of reinforced concrete structures with external steel shear walls. J Constr Steel Res 70:226–235. https://doi.org/10.1016/j.jcsr.2011.08.010

Hayashi T, Niwa H, Fukuhara M (1980) Strengthening methods of the existing reinforced concrete buildings. In: Proceedings of the 7th world conference on earthquake engineering, Istanbul, vol 4, pp 89–97

Higashi Y, Endo T, Ohkubo M, Shimizu Y (1980) Experimental study on strengthening reinforced concrete structure by adding shear wall. In: Proceedings of the 7th world conference on earthquake engineering, Istanbul, pp 173–180

Husain M, Eisa AS, Hegazy MM (2019) Strengthening of reinforced concrete shear walls with openings using carbon fiber-reinforced polymers. Int J Adv Struct Eng. https://doi.org/10.1007/s40091-019-0216-6

Inukai M, Kaminosono T (2000) Seismic performance of an existing RC frame retrofitted by precast prestressed concrete shear walls. In: 12th world conference on earthquake engineering, 2000, paper no. 2246

Kahn LF, Hanson R (1979) Infilled walls for earthquake strengthening. ASCE J Struct Div 105(2):283–296

Kaltakci MY, Ozturk M (2012) An experimental study on the strengthening of non-ductile reinforced concrete frames via external shear wall. Eur J Environ Civ Eng 16(1):59–76

Kaltakci MY, Yavuz G (2014) The seismic improvement and control of weak concrete frames with partial concrete shear walls. J Vib Contr 20(8):1239–1256. https://doi.org/10.1177/1077546312467220

Kaltakci MY, Arslan MH, Yilmaz SU, Arslan HD (2008) A new approach on the strengthening of primary school buildings in Turkey: an application of external shear wall. Build Environ 43(6):983–990. https://doi.org/10.1016/j.buildenv.2007.02.009

Kaltakci MY, Ozturk M, Arslan MH (2010) An experimental investigation for external RC shear wall applications. Nat Hazards Earth Syst Sci 10(9):1941–1950. https://doi.org/10.5194/nhess-10-1941-2010

Kaplan H, Nohutcu H, Cetinkaya N, Yılmaz S, Gonen H, Atımtay E (2009) Seismic strengthening of pin connected precast concrete structures with external shear walls and diaphragms. PCI J 54(1):88–99

Kaplan H, Yılmaz S, Cetinkaya N, Atımtay E (2011) Seismic strengthening of RC structures with exterior shear walls. Sadhana, Acad Proc Eng Sci 36:17–34. https://doi.org/10.1007/s12046-011-0002-z

Karadogan HF, Pala S, Ilki A, Yüksel E, Mowrtage W, Teymur P et al (2009) Improved infill walls and rehabilitation of existing low rise buildings. Seismic Risk Assess Retrofit. Springer, Dortrecht, pp 387–426

Kucukgoncu H (2018) An experimental study of analyzing the seismic behaviour of strengthened three dimensional frame structure. PhD thesis, Erciyes University Graduate School of Natural and Applied Science, Turkey

Lombard J, Humar JL, Cheung MS (2000) Seismic strengthening and repair of reinforced concrete shear walls. In: 12th World conference on earthquake engineering, 2000, paper no. 2032

Pincheira JA, Jirsa JO (1995) Seismic response of RC frames retrofitted with steel braces or walls. J Struct Eng 121(8):1225–1235. https://doi.org/10.1061/(ASCE)0733-9445(1995)121:8(1225)

Pujola S, Fick D (2010) The test of a full-scale three-story RC structure with masonry infill walls. Eng Struct 32(10):3112–3121. https://doi.org/10.1016/j.engstruct.2010.05.030

Rodriguez M, Eeri M, Park R (1991) Repair and strengthening of reinforced concrete buildings for seismic resistance. Earthq Spect 7(3):439–457

Sacco E, Serpieri R, Alfano G (2017) Multiplane cohesive zone models combining damage, friction and interlocking. In: Models, simulation, and experimental issues in structural mechanics. Springer, Cham, pp 61–86

SAP 2000 (2017) Integrated structural analysis and design software, Ver. 19.0.0, Computers and Structures, Inc., Berkeley, CA, USA

Solak A, Tama YS, Yılmaz S, Kaplan H (2015) Experimental study on behavior of anchored external shear wall panel connections. Bull Earthq Eng 13(10):3065–3081. https://doi.org/10.1007/s10518-015-9748-8

TEC (2007) Turkish earthquake code: specifications for the buildings to be constructed in disaster areas. In: Official Gazette no 26454. Ankara

Tezcan SS, Ikizogulları S (1998) Stresses along the periphery of the infilled shear walls in retrofitted frames. In: Repair and strengthening of existing buildings. Second Japan-Turkey workshop on earthquake engineering, İstanbul, Turkey, pp. 199–209

Tsionis G, Taucer F, Pinto A (2015) Seismic strengthening of RC frames with shear walls. In: Proceedings of the 6th international conference on mechanics and materials in design, P. Delgada/Azores, 2015, paper no. 5669

Yüksel E, Ilki A, Erol G, Demir C, Karadogan HF (2006) Seismic retrofit of infilled reinforced concrete frames with CFRP composites. Seismic Assessment and Rehabilitation of Existing Buildings, Nato SFP: 977231, International Advanced Research Workshop, Istanbul, Turkey, 2006. https://doi.org/10.1007/s40091-018-0207-z